Original paper

Contribution to the crystallography of hydrotalcites: the crystal structures of woodallite and takovite

Stuart J. MILLS[1,2*], Pamela S. WHITFIELD[3], Anthony R. KAMPF[4], Siobhan A. WILSON[1,5], Gregory M. DIPPLE[1], Mati RAUDSEPP[1], Georges FAVREAU[6]

[1] *Mineral Deposit Research Unit, The University of British Columbia, Vancouver, British Columbia, Canada V6T 1Z4*
[2] *Geosciences, Museum Victoria, GPO Box 666, Melbourne 3001, Victoria, Australia; smills@museum.vic.gov.au*
[3] *Institute for Chemical Process and Environmental Technology, National Research Council of Canada, Montréal Road, Ottawa, Ontario, Canada K1A 0R6*
[4] *Mineral Sciences Department, Natural History Museum of Los Angeles County, 900 Exposition Boulevard, Los Angeles, California 90007, U.S.A.*
[5] *School of Geosciences, Monash University, Clayton 3800, Victoria, Australia*
[6] *421 Avenue Jean Monnet, 13090 Aix-en-Provence, France*
[*] *Corresponding author*

The crystal structures of the 3*R* polytypes of takovite and woodallite are presented. The structure of takovite was solved on a single crystal from the Agoudal mine, Bou Azzer district, Tazenakht, Morocco to R_1 = 1.87 % for 94 unique reflections [$F_o > 4\sigma F$] in $R\bar{3}m$, with unit cell parameters a = 3.0290(2) and c = 22.5995(15) Å. The crystal structure of woodallite [space group $R\bar{3}m$, with unit cell parameters a = 3.10124(8) and c = 23.6817(16) Å] was refined utilising the Rietveld method on a sample from the MKD5 orebody at the Mount Keith Nickel Mine, Western Australia.

Keywords: hydrotalcite, layered double hydroxide, takovite, woodallite, crystal structure, Rietveld refinement
Received: 27 June 2012; accepted: 14 December 2012; handling editor: F. Laufek

1. Introduction

Members of the hydrotalcite supergroup have the general formula $A_{6-x}B_{2+x}(OH)_{16}X{\cdot}nH_2O$, which is based on positively charged brucite-like layers $(A_{6-x}B_{2+x})(OH)_2$, where A is a divalent cation (e.g., Mg^{2+}, Fe^{2+}, Mn^{2+}, Ni^{2+} and Cu^{2+}) and B is a trivalent cation (e.g., Al^{3+}, Fe^{3+}, Cr^{3+}, Mn^{3+} and Ga^{3+}). Interlayer regions typically contain a monovalent or divalent anion X, such as CO_3^{2-}, SO_4^{2-}, Cl^-, and OH^-. Other anions or a combination of anions may compensate for the positive charge of the brucite-like layers. Water molecules and occasional cations may also be present within the interlayer (Drits et al. 1987; Bookin and Drits 1993). There are more than 40 natural members of the group (Mills et al. 2012), and an extensive list of synthetic analogues, termed "layered double hydroxides" (LDHs) or hydrotalcite-like compounds. Several books have also been dedicated to this topic (e.g., Duan and Evans 2006). Layered double hydroxides are very important to industry, and have found uses as catalysts, drug delivery media, and sequestering agents for organic polymers and CO_2 (Duan and Evans 2006; Kameda et al. 2011).

Woodallite, ideally $Mg_6Cr_2(OH)_{16}Cl_2{\cdot}4H_2O$, was described by Grguric et al. (2001) from the Mount Keith mine, Western Australia, as the Cr-analogue of iowaite ($Mg_6Fe_2(OH)_{16}Cl_2{\cdot}4H_2O$). The woodallite crystals contain substantial Fe^{3+} and Al^{3+} substitution with the empirical formula: $Mg_{6.19}(Cr^{3+}_{1.21}Fe^{3+}_{0.51}Al^{3+}_{0.15})_{\Sigma 1.87}(OH)_{16}[Cl_{1.62}(CO_3)_{0.17}(SO_4)_{0.01}]{\cdot}4H_2O$, indicating partial substitution towards iowaite and the hypothetical mineral $Mg_6Al_2(OH)_{16}Cl_2{\cdot}4H_2O$ (Grguric et al. 2001). Woodallite crystals are typically curved and intergrown and less than 10 μm in size, and thus are not suitable for single crystal investigation. Grguric et al. (2001) instead indexed the powder pattern in the space group $R\bar{3}m$ with the unit cell a = 3.103(2), c = 24.111(24) Å, V = 201.14 Å^3 and $Z = {}^3/_8$.

Takovite, $Ni_6Al_2(OH)_{16}CO_3{\cdot}4H_2O$, was originally described by Maksimović (1957) from Takovo, Serbia and reinvestigated by Bish and Brindley (1977) on samples from the type locality as well as from the Perseverance mine, Western Australia and Cap Garonne, France. Bish and Brindley (1977) reported the following rhombohedral unit cell parameters (no space group was noted) based on powder diffraction for Serbian takovite: a = 3.0250(1), c = 22.595(3) Å, V = 179.06(2) Å^3 and Western Australian takovite: a = 3.0280(4), c = 22.45(2) Å and V = 178.31(15) Å^3.

Due to the limited information on the structure of the two minerals and their polytypes, and as part of

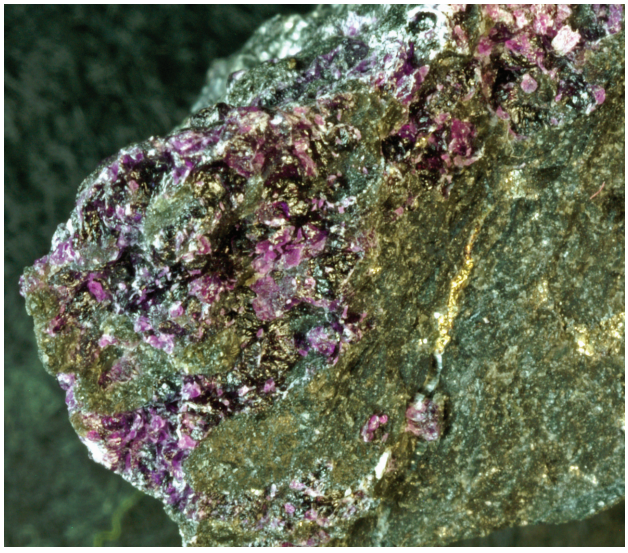

Fig. 1 Lilac coloured woodallite in greenish komatiite with pyrrhotite. Museum Victoria specimen M48643. Photograph John Bosworth. Field of view approximately 3 cm across.

our recent related studies (Mills et al. 2011) and the nomenclature of the supergroup (Mills et al. 2012), we decided to tackle the structures of both woodallite and takovite. The crystal structure results are reported herein.

2. Sample descriptions

2.1. Woodallite

Woodallite forms as a constituent of the MKD5 orebody at the Mount Keith Nickel Mine in the North Eastern Goldfields district of Western Australia (Fig. 1). The woodallite used in this study was extracted from the tailings found at the mine. The tailings consist primarily of antigorite and lizardite with hydrotalcite-group

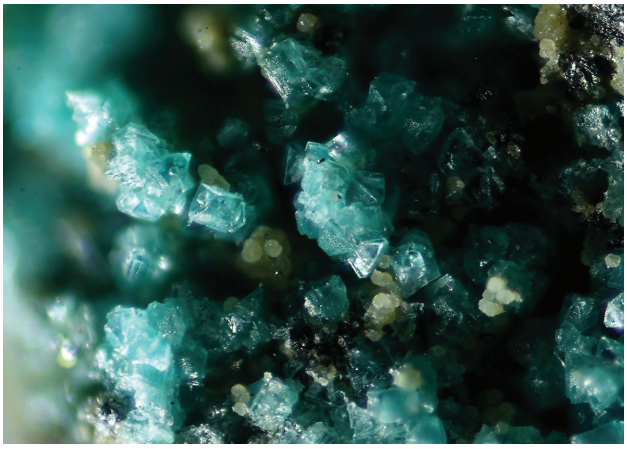

Fig. 2 Green takovite crystals with tan balls of a saponite-like mineral. Specimen and image Georges Favreau. Field of view approximately 3 mm.

Tab. 1 Data collection and structure refinement details for takovite

Simplified formula	$Ni_6Al^{3+}_2(OH)_{16}[CO_3]\cdot 4H_2O$
Temperature	296(2) K
Wavelength	0.71075 Å
Space group	$R\bar{3}m$
Unit cell dimensions	a = 3.0290(2) Å
	c = 22.5995(15) Å
Volume	179.57(2) Å^3
Z	$^3/_8$
Absorption coefficient	5.372 mm^{-1}
F(000)	148
Theta range for data collection	2.70 to 29.87°
Index ranges	$-3 \le h \le 4$, $-4 \le k \le 4$, $-30 \le l \le 30$
Reflections/unique	1606 / 94 [R_{int} = 0.0212]
Refinement method	Full-matrix least-squares on F^2
Data/restraints/parameters	94 / 1 / 17
Goodness-of-fit on F^2	1.224
Final R indices [$I>4\sigma(I)$]	R_1 = 0.0187, wR_2 = 0.0187
R indices (all data)	R_1 = 0.0452, wR_2 = 0.0452
Extinction coefficient	0.0000(5)
Largest diff. peak and hole	1.04 and –0.19 e/Å^3

Tab. 2 Atom coordinates and isotropic displacement parameters (Å^2) for takovite

Atom	*x*	*y*	*z*	Occupancy	U_{eq}	U_{11}	U_{22}	U_{33}	U_{23}	U_{13}	U_{12}
Ni	0	0	0	0.623(11)	0.0095(3)	0.0077(3)	0.0077(3)	0.0132(4)	0	0	0.00387(16)
Al	0	0	0	0.377(11)	0.0095(3)	0.0077(3)	0.0077(3)	0.0132(4)	0	0	0.00387(16)
O1	$^1/_3$	$^2/_3$	0.04374(9)	1	0.0160(7)	0.0178(8)	0.0178(8)	0.0124(10)	0	0	0.0089(4)
H1	$^1/_3$	$^2/_3$	0.0822(11)	1	0.019(4)						
O2	0.168(7)	0.168(7)	$^1/_2$	0.17	0.036(7)	0.040(6)	0.040(6)	0.022(2)	–0.0006(15)	0.0006(15)	0.015(5)
C	0.3333	0.6667	0.4992(16)	0.17	0.063(12)	0.074(18)	0.074(18)	0.040(14)	0	0	0.037(9)

minerals (i.e. iowaite and woodallite with uncommon pyroaurite, stichtite, and mountkeithite). Minor brucite, talc, magnetite, chromite, quartz, magnesite, dolomite, calcite and trace vermiculite with Ni-, Fe- and Cu-sulphide minerals are common (e.g., Wilson 2009; Mills et al. 2011). More details on the quantification of the tailings can be found in Mills et al. (2010).

2.2. Takovite

A small block collected in the ore piles from the Agoudal mine, Bou Azzer district, Tazenakht, Morocco, appeared very rich in fine-grained metallic minerals, and was shot through with pale green veinlets. These contained numerous columnar crystals of takovite up to *c.* 0.3 mm across. Crystals are either isolated or intergrown in coatings, and exhibit triangular/hexagonal pinacoids with a pearly lustre (Fig. 2). The takovite occurs in a matrix consisting mostly of skutterudite (massive and in silver-white crystals), alloclasite (massive and black) and orthoclase (massive, tan to pink). Tan balls of a Ni–Al silicate that seems to be related to saponite are found growing on the takovite, and a mineral related to nimite is also associated. Older specimens collected in the Bou Azzer district at Aghbar in the 1960's by Jacques Dietrich show similar crystals. These, however, were described as "chalcophyllite" by Favreau and Dietrich (2001). To our knowledge, these takovite crystals from Agoudal are the best for the species (i.e. crystal size, morphology and crystal quality).

3. Experimental methods

3.1. X-ray crystallography

Single-crystal X-ray diffraction data for takovite were obtained at 296(2) K on a Rigaku R-Axis Rapid II curved imaging plate microdiffractometer utilising monochromatised MoK_α radiation. The Rigaku CrystalClear software package was used for processing the structure data, including the application of shape-based

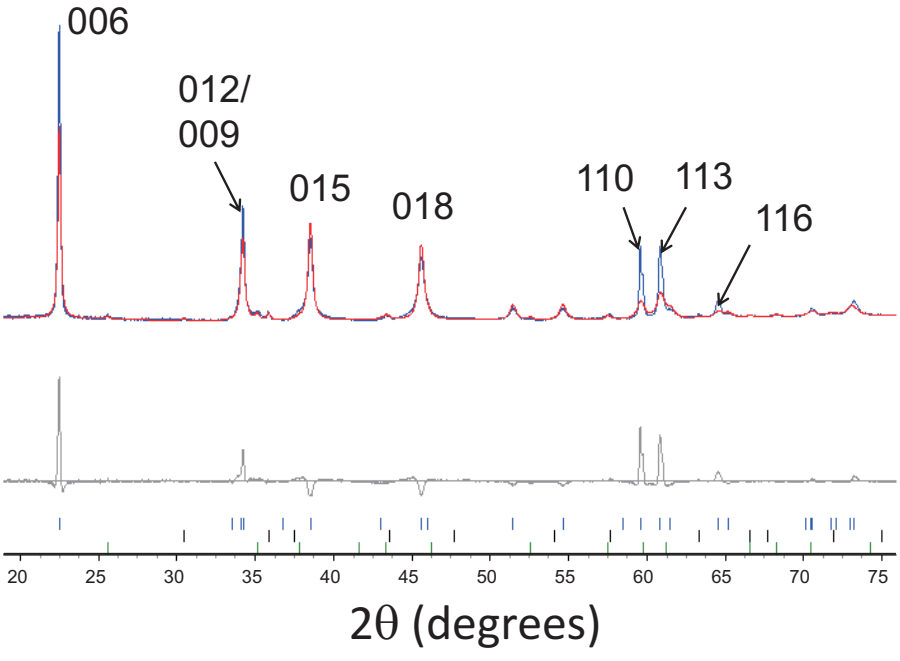

Fig. 3 Pawley fit to the woodallite data up to approximately 75 degrees 2θ. The intensity in this plot is on a square-root scale and the Miller indices of the major reflections are indicated. The difference plot clearly shows the presence of anisotropic broadening and no significant peak shifts.

Tab. 3 Variable count and step data collection regime for woodallite

Angular range (2θ)	Counting time (s)	Step size (°)
9–29	6	0.0142
29–62.7	9	0.0214
62.7–90	15	0.0285
90–140	21	0.0356

and empirical absorption corrections. The structure was solved in space group $R\bar{3}m$ (No. 166), by direct methods using SHELXL-97 (Sheldrick 2008) and subsequent Fourier and difference Fourier syntheses, followed by anisotropic full-matrix least-squares refinements on F^2 using SHELXL-97. The final model for the refinement (with H atom determined) converged to R_1 = 1.87 % for 94 unique reflections [$F_o > 4\sigma F$]. The refinement details are given in Tab. 1 and the refined atomic coordinates, site occupancies and displacement parameters are given in Tab. 2.

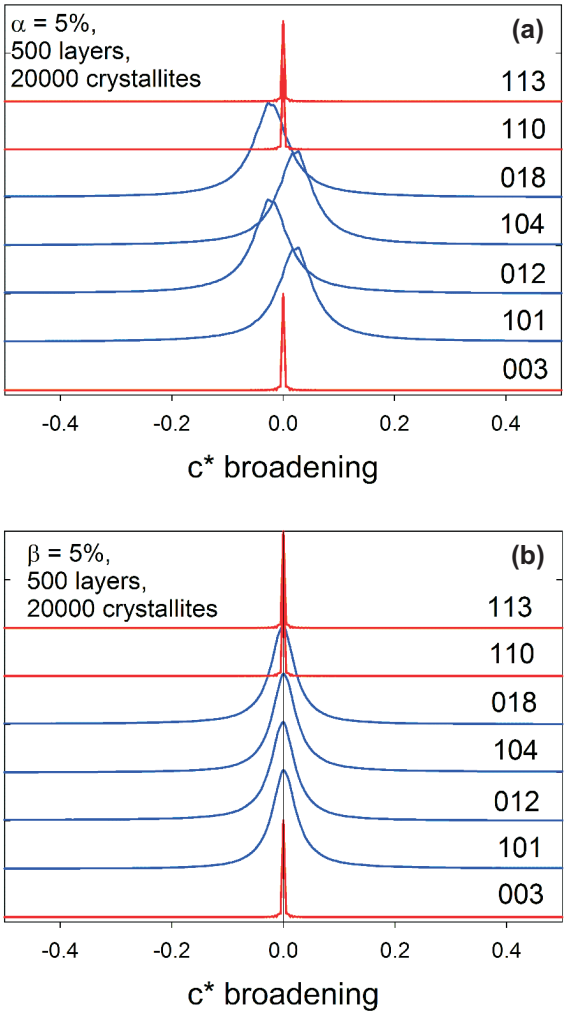

Fig. 4 Results from a Monte Carlo simulation (Whitfield et al. 2005) to show broadening along the *c** reciprocal lattice direction in a cubic close-packed structure with (**a**) 5% stacking faults and (**b**) 5% twinning faults.

3.2. Rietveld refinement

Samples of woodallite were mounted in 0.5 mm quartz capillaries. The data were collected on a Bruker D8 Advance CuK_α diffractometer with a focusing primary mirror and a VÅNTEC position sensitive detector (PSD). Due to the small sample size, a 8 mm Debye slit was used to reduce scattering from the empty capillary. Both conventional and pseudo-variable count-time (VCT) data sets (Madsen and Hill 1994) were obtained from the sample. The VCT data collection tries to compensate for the X-ray form factor drop off at high angles by counting longer at higher angles. Improving the contribution of the higher order reflections in a refinement improves the precision and accuracy that may be obtained (Madsen and Hill 1994). The original VCT methodology with a point detector and continually varying count times cannot be done using a PSD detector. Pseudo-VCT data can be obtained by dividing the complete pattern into sections and increasing the count-time accordingly in each one. There is also the opportunity to shorten the experiment by increasing the step size with angle at the same time. The data collection regime used is shown in Tab. 3. The data were merged into a *.xye* file and a blank capillary background subtracted whilst retaining the correct counting statistics. To prevent the least-squares refinement from being dominated by the intense, low-angle reflections, an additional weighting was added into the refinement to enhance the contribution of the weaker, higher order reflections beyond that from the VCT data collection. Analysis of the data was undertaken using the TOPAS software, version 4.1 (Bruker AXS 2008).

A Pawley unit-cell refinement in TOPAS showed that woodallite exhibits anisotropic peak broadening as shown in Fig. 3. Such broadening is not unexpected in a layered structure, but it can be problematic. The behaviour of faulted systems was described by Warren (1969). The effects on the diffraction positions and profiles differ depending on whether the stacking is hexagonal (*hcp*) or cubic close-packed (*ccp*). In *hcp* structures both stacking and twinning faults cause only broadening of selected reflections. In *ccp* structure twinning faults produce similar broadening to *hcp* structures but stacking faults cause peak shifts and asymmetry in addition to broadening. The different behaviour is illustrated in Fig. 4 using results along the *c** reciprocal space direction from a Monte Carlo simulation (Whitfield et al. 2005). If a reflection satisfies the rule $h - k = 3n$, then it is broadened. The $R\bar{3}m$ polytype of woodallite has a *ccp* structure, but the absence of significant systematic peak shifts and asymmetry in the diffraction suggests that the major source of the broadening in woodallite is twinning faults. This is fortunate as the macro code for *ccp* stacking fault effects

Tab. 4 Atom coordinates and isotropic displacement parameters ($Å^2$) for woodallite

atom	*x*	*y*	*z*	occupancy	B_{iso}
Mg1	0	0	0	0.75	1.06(6)
Cr	0	0	0	0.124	1.06(6)
Al	0	0	0	0.039	1.06(6)
Fe	0	0	0	0.087	1.06(6)
O1	$^1/_3$	$^2/_3$	0.041590(94)	1	1.06(6)
H1	$^1/_3$	$^2/_3$	0.08168(92)	1	1.06(6)
O2	0.3378(17)	0.3378(17)	$^1/_2$	0.1419(16)	2.0(3)
C1	0	0	$^1/_2$	0.07	2.0(3)
Cl1	0	0	$^1/_2$	0.11	2.0(3)

Occupancy parameters for Mg, Cr, Al and Fe were taken from the chemical composition

have not been worked out in TOPAS yet. The selection rule for twinning faults in a *ccp* structure is the same as for *hcp*, so empirically (but not for a quantitative microstructure analysis) the *hcp* model will fit pure twinning faults in a *ccp* phase.

A model developed for work on lithium battery materials (Whitfield et al. 2005) was successfully used to empirically model the broadening during the structure refinement. It is a reciprocal space relationship that is functionally equivalent to the Warren (1969) *hcp* faulting model, but only requires a single variable. Using spherical harmonics to convolute an additional Lorentzian into the diffraction profile can also achieve a similar fit, however, this requires many more variables to reach the same result.

Since hydrotalcites have mixed and partially occupied sites, some form of constraint must be used to produce meaningful results from a single diffraction dataset. The composition of woodallite is variable; however, by fixing the carbonate content to 0.17 *apfu*, as shown in the original analyses, a refinement with a good fit, and a refined composition close to that expected, were obtained.

The structure of woodallite was expected to be the same as that of its Fe-containing analogue iowaite (Braithwaite et al. 1994), with Cl disordered over the 18*g* site. However, using the iowaite structure produced a very poor fit to the data. The need to take into account additional scattering from residual carbonate in the woodallite reveals a problem when trying to disorder CO_3 and

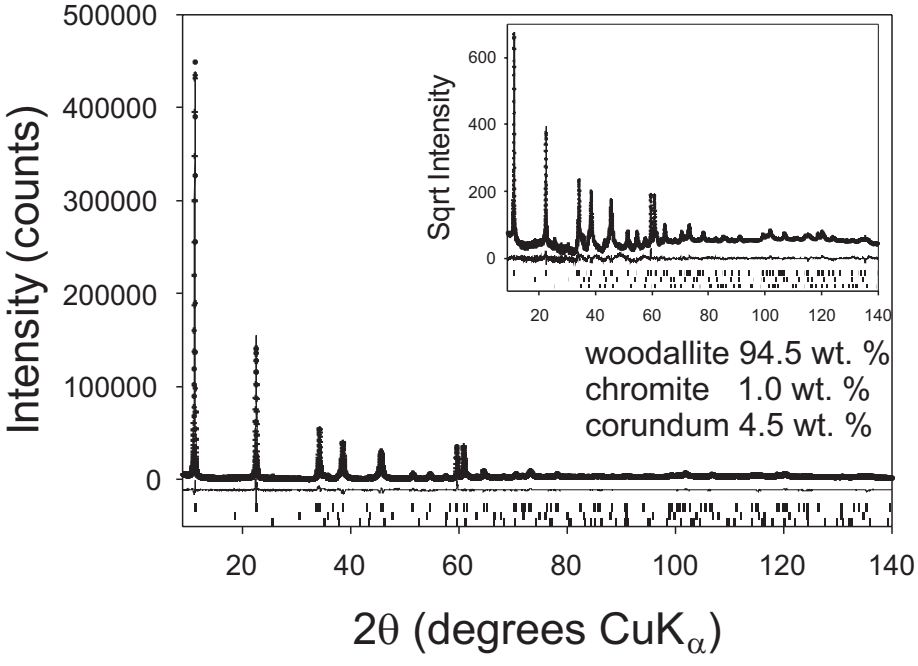

Fig. 5 Difference plot for the Rietveld refinement of woodallite. Inset is the fit with intensity on a square-root scale to exaggerate the weaker high-angle reflections. The relatively high R_{wp} of 14 % reflects the highly constrained nature of the model, low background, residual profile problems and difficulties with the fitting the background that are more obvious on the square-root scale plot. A Le Bail fit yields a R_{wp} of 6.4 % with the same data which is quite high for VCT data.

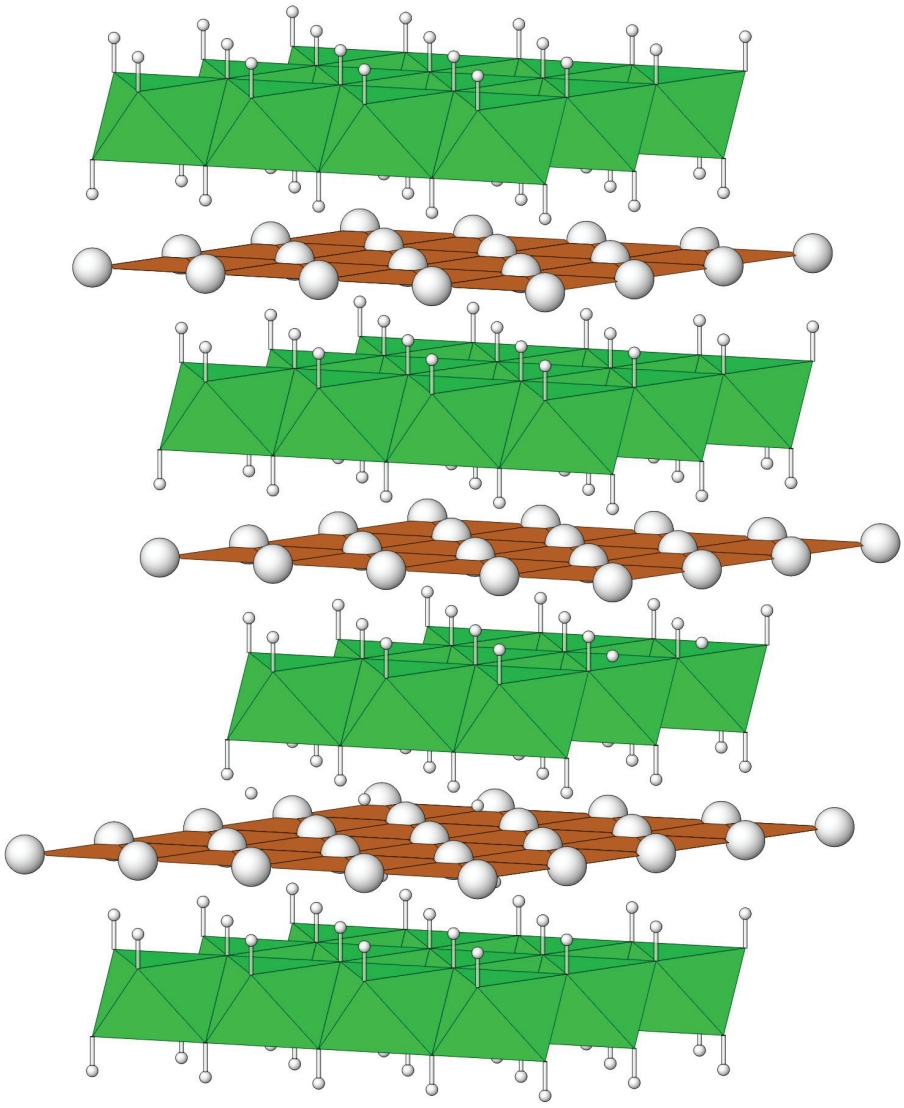

Fig. 6 The crystal structure of takovite (3*R* polytype) shown in clinographic projection. The (Ni,Al) octahedra are green, edge-sharing CO_3 triangles orange, H are small grey spheres and O of H_2O large grey spheres. Note that all CO_3 triangles are shown, however, they are only partially occupied.

Cl around the same site. The general site multiplicity around the iowaite 18*g* site is 36, which makes locating a CO_3 group not impossible but somewhat clumsy. On the basis of difference map studies, it was hypothesized that the 18*g* site was occupied by the oxygen atoms of the CO_3 group and that Cl shared the 3*b* site with the C atom (Tab. 4). This model produced a good fit to the data as shown in Fig 5. The carbonate oxygen position was refined with a C–O bond distance restraint to maintain a sensible structure given the small site occupancy. The final refinement converged to R_p = 8.95 and R_{wp} = 14.68. The fit is not perfect as expected from a highly constrained model and ignoring the inevitable profile contribution from a smaller but finite fraction of stacking faults. High-quality, low-noise data also tend to increase the difference between R_{exp} and R_{wp} as the uncertainties in the intensities are reduced compared to the effect of even minor imperfections in fitting (Toby 2006). Counting statistics generally follow as square-root of intensities. The square-root inset in Fig. 5 does not show any large discrepancies in the difference plot other than background fitting issues *c.* 45–50 degrees 2θ.

4. Discussion of the structures

The hydrotalcite group is notable for its wide range of polytypism, which includes a number of *H* = hexagonal and *R* = rhombohedral polytypes. The nature of this polytypism was discussed in detail by Bookin and Drits (1993), Bookin et al. (1993a, b) and, more recently, by Evans and Slade (2006) and Mills et al. (2012). In terms of polytypism, both woodallite and takovite may be considered 3*R* polytypes, with a $3R_1$ stacking sequence (Fig. 6). No superstructure reflections were observed for non-integral *h* or *k*, implying that $a \approx 3$ Å and that there is no long-range order within the layers of the structure, or at least, no registration of any long-

range order. For takovite, this confirms the stacking sequence put forward by Bookin et al. (1993a) and confirms the most symmetrical possible space group for the mineral.

For woodallite, these results confirm the space group assigned by Grguric et al. (2001), and, more importantly, indicate the possibility of complete solid solution between the end-members woodallite and stichtite. Woodhouse (2006) showed ion exchange between CO_3 and Cl to occur in synthetic samples of woodallite and stichtite. The 3*R* polytype with no superstructure is common within the natural LDH minerals (e.g. Mills et al. 2012).

Acknowledgements. Andrew Christy, two anonymous referees and Associate Editor František Laufek are thanked for helpful comments on the manuscript. The support of the Natural Sciences and Engineering Research Council of Canada (NSERC) through a Collaborative Research and Development Grant to GMD and a Discovery Grant to MR is acknowledged. SAW was supported by a Foundation Scholarship from the Mineralogical Association of Canada and an Alexander Graham Bell Canada Graduate Scholarship from NSERC. Part of this study was also funded by the John Jago Trelawney Endowment to the Mineral Sciences Department of the Natural History Museum of Los Angeles County.

References

Bish DL, Brindley GW (1977) Reinvestigation of takovite, a nickel aluminium hydroxy-carbonate of the pyroaurite group. Amer Miner 62: 458–464

Bookin AS, Drits VA (1993) Polytype diversity of the hydrotalcite-like minerals. I. Possible polytypes and their diffraction features. Clays and Clay Miner 41: 551–557

Bookin AS, Cherkashin VI, Drits VA (1993a) Polytype diversity of the hydrotalcite-like minerals. II. Determination of the polytypes of experimentally studied varieties. Clays and Clay Miner 41: 558–564

Bookin AS, Cherkashin VI, Drits VA (1993b) Reinterpretation of the X-ray diffraction patterns of stichtite and reevesite. Clays and Clay Miner 41: 631–634

Braithwaite RSW, Dunn PJ, Pritchard RG, Paar WH (1994) Iowaite, a re-investigation. Mineral Mag 58: 79–85

Bruker (2008) SAINT, SADABS AND SHELXTL. Bruker AXS Inc. Madison, Wisconsin, USA

Drits VA, Sokolova TN, Sokolova GV, Cherkashin VI (1987) New members of the hydrotalcite–manasseite group. Clays and Clay Miner 35: 401–417

Duan X, Evans DG (eds) (2006) Layered double hydroxides. Structure and Bonding 119 (Special volume): 1–234

Evans DG, Slade RCT (2006) Structural aspects of layered double hydroxides. Structure and Bonding 119: 1–87

Favreau G, Dietrich JE (2001) Le district cobalto-nickélifère de Bou Azzer (Maroc) – Géologie, histoire et description des espèces minérales. Le Cahier des Micromonteurs 3: 1–115

Grguric BA, Madsen IC, Pring A (2001) Woodallite, a new chromium analogue of iowaite from the Mount Keith nickel deposit, Western Australia. Mineral Mag 65: 427–435

Kameda T, Uchiyama N, Yoshioka T (2011) Removal of HCl, SO_2, and NO by treatment of acid gas with Mg–Al oxide slurry. Chemosphere 82: 587–591

Madsen IC, Hill RJ (1994) Collection and analysis of powder diffraction data with near-constant counting statistics. J Appl Cryst 27: 385–392

Maksimović Z (1957) Takovite, hydrous nickel aluminate, a new mineral. Zapisnici Srpskog geološkog društva 1955: 219–224

Mills SJ, Wilson SA, Dipple GM, Raudsepp M (2010) The decomposition of konyaite: importance in CO_2 fixation in mine tailings. Mineral Mag 74: 903–917

Mills SJ, Whitfield PS, Wilson SA, Woodhouse JN, Dipple GM, Raudsepp M, Francis CA (2011) The crystal structure of stichtite, re-examination of barbertonite and the nature of polytypism in MgCr hydrotalcites. Amer Miner 96: 179–187

Mills SJ, Christy AG, Génin J-MR, Kameda T, Colombo F (2012) Nomenclature of the hydrotalcite supergroup: natural layered double hydroxides. Mineral Mag 76: 1289–1336

Sheldrick GM (2008) SHELXL97 – program for the refinement of crystal structures. University of Göttingen, Germany

Toby BH (2006) R factors in Rietveld analysis: how good is good enough? Powder Diffr 21: 67–70

Warren BE (1969) X-ray Diffraction. Dover Publications Inc, New York, USA, pp 381

Whitfield PS, Niketic S, Le Page Y, Davidson IJ (2005) Investigating the nature of line broadening in electrochemically delithiated $Li_{1.2}Mn_{0.4}Ni_{0.3}Co_{0.2}O_2$. Advances in X-ray Analysis 49: 149–155

Wilson SA (2009) Mineral Traps for Greenhouse Gases in Mine Tailings: a Protocol for Verifying and Quantifying CO_2 Sequestration in Ultramafic Mines. Unpublished Ph.D. Thesis, University of British Columbia, Vancouver, BC, Canada, pp 1–315

Woodhouse JN (2006) The Characterization of Hydrotalcite-Group Minerals and Their Anion Exchange Capabilities at Mount Keith Nickel Mine, Western Australia. Unpublished B.Sc. Thesis, University of British Columbia, Vancouver, BC, Canada, pp 1–72